



$[closo-1-CB_{11}H_{11}-1-Ph]^-$ as a structural element for ionic liquid crystals



Aleksandra Jankowiak^a, Junichiro Kanazawa^{a,b}, Piotr Kaszynski^{a,c,*}, Ryo Takita^b, Masanobu Uchiyama^b

^a Organic Materials Research Group, Department of Chemistry, Vanderbilt University, Nashville, TN 37235, USA

^b Graduate School of Pharmaceutical Sciences, The University of Tokyo, 7-3-1 Hongo, Bunkyo-ku, Tokyo 113-0033, Japan

^c Section of Heteroorganic Compounds, University of Łódź, Tamka 12, 91403 Łódź, Poland

ARTICLE INFO

Article history:

Received 20 March 2013

Received in revised form

23 May 2013

Accepted 24 May 2013

Dedicated to Professor Vladimir Bregadze on the occasion of his 75th birthday.

Keywords:

Boron clusters

Ion pairs

Liquid crystals

Structure–property relationship

ABSTRACT

Ion pairs **2[Pyrr]** and **3[Pyrr]** containing $[closo-1-CB_{11}H_{11}-1-Ph]^-$ as the structural element were synthesized and their liquid crystalline properties were investigated by thermal and optical methods. Their mesogenic behavior was compared to that of the analogous series **1[Pyrr]** having a COO linking group between the benzene ring and the cluster, and the observed structure–property relationships are discussed in the context of general trends in related non-ionic liquid crystals.

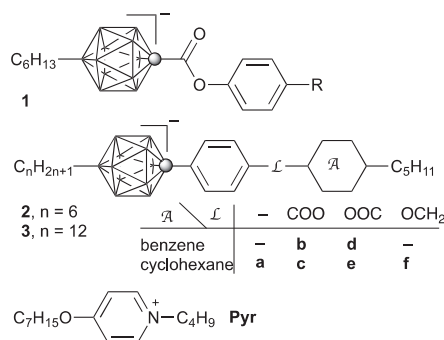
© 2013 Elsevier B.V. All rights reserved.

1. Introduction

A recently developed method for C-arylation of the $[closo-1-CB_{11}H_{12}]^-$ cluster **1** has opened up possibilities for synthesis of new materials with improved properties. One such class of materials are ionic liquid crystals (ILC), in which the mesogenic properties are driven by the anisometric anion. These compounds are capable of anisotropic cation transport [2–6] and are of interest for ion batteries [7] and solar cell applications [8]. In this context we have demonstrated that *closo*-carborates $[closo-1-CB_9H_{10}]^-$ (**A**, Fig. 1) and $[closo-1-CB_{11}H_{12}]^-$ (**B**) are suitable structural elements for ILC, such as **IA** and **IB** in Fig. 1 [9–11], and ion pairs **1[Pyrr]** containing $[closo-1-CB_{11}H_{12}]^-$ (**B**), exhibit SmA and nematic phases [11]. The new synthetic method [1] opens access to C-aryl derivatives of cluster **B** and enables synthesis of new series of ILC such

as **2[Pyrr]** and **3[Pyrr]**, including those lacking the ester group and, consequently, with increased chemical stability. The first two members of this new family of ILC, **2c[Pyrr]** and **2f[Pyrr]**, were reported recently [1].

Here we describe the synthesis and characterization of mesogenic ion pairs **2[Pyrr]**, derived from the $[closo-1-CB_{11}H_{11}-1-Ph]^-$, with the C_6H_{13} chain and one derivative **3c[Pyrr]** with double length of the alkyl chain. Properties of the new compounds are compared to those of series **1[Pyrr]** and are used for structure–property relationship analysis.



* Corresponding author. Organic Materials Research Group, Department of Chemistry, Vanderbilt University, Box 1822 Station B, Nashville, TN 37235, USA. Tel.: +1 615 322 3458; fax: +1 615 343 1234.

E-mail addresses: aleksandra.jankowiak@Vanderbilt.Edu (A. Jankowiak), 1727407712@mail.ecc.u-tokyo.ac.jp (J. Kanazawa), piotr.kaszynski@vanderbilt.edu (P. Kaszynski), takita@mol.f.u-tokyo.ac.jp (R. Takita), uchiyama@mol.f.u-tokyo.ac.jp (M. Uchiyama).

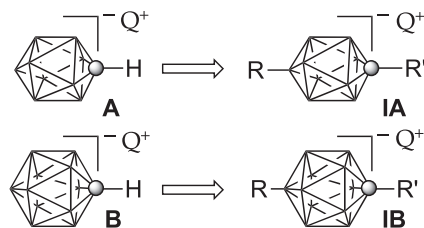


Fig. 1. The structures of the [closo-1-CB₉H₁₀]⁻ (A) and [closo-1-CB₁₁H₁₂]⁻ (B) clusters, and ion pairs of their 1,10- (IA) and 1,12-disubstituted (IB) derivatives with the counterion Q⁺. Each vertex represents a BH fragment and the sphere is a carbon atom.

2. Results and discussion

2.1. Synthesis

Esters **1b**, **1d**, **2b**, **2c**, and **3c** were prepared from appropriate carboxylic acids **4**[NET₄]⁺–**6**[NET₄]⁺. Thus, carboxylic acids were converted to acid chlorides with (COCl)₂ and treated with appropriate phenol **7** or *trans*-4-pentylcyclohexanol (**8**) to give desired esters as the [NET₄]⁺ salts (Scheme 1). The reaction with the cyclohexanol was conducted with five-fold excess alcohol, and at high concentration and temperature to assure formation of the esters. Esters **2d**[NMe₄]⁺ and **2e**[NMe₄]⁺ were obtained by esterification of phenol **9**[NMe₄]⁺ with 4-pentylbenzoyl chloride and *trans*-4-pentylcyclohexanecarbonyl chloride, respectively (Scheme 2). Finally, alkylation of phenol **9**[NMe₄]⁺ with tosylate **10** [13] in DMF in the presence of K₂CO₃ resulted in derivative **2f**[NMe₄]⁺ isolated in 76% yield. The ion pairs **1**[Pyr]–**3**[Pyr] were prepared by exchange of the [NET₄]⁺ or [NMe₄]⁺ cation for *N*-butyl-4-heptyloxypyridinium [9,14] (Pyr) in a biphasic CH₂Cl₂/H₂O system following the procedure previously reported for the preparation of ion pair **1a**[Pyr] [11].

Carboxylic acid **6**[NET₄]⁺ was obtained by Negishi coupling [15,16] of iodo acid [closo-1-CB₁₁H₁₀-1-(4-C₆H₄COOH)-12-I]⁻ [NMe₄]⁺ (**11** [NMe₄]⁺) [1] with 12-fold excess dodecylzinc chloride in the presence of Pd(0) and PCy₃ ligand generated *in-situ* (Scheme 3), as described previously for the preparation of acids [closo-1-CB₁₁H₁₀-1-COOH-12-C₆H₁₃]⁻ [NMe₄]⁺ (**4**[NMe₄]⁺) [11] and [closo-1-CB₁₁H₁₀-1-(4-C₆H₄COOH)-12-C₆H₁₃]⁻ [NET₄]⁺ (**5**[NET₄]⁺) [1]. A similar Negishi coupling of iodo phenol [closo-1-CB₁₁H₁₀-1-(4-C₆H₄OH)-12-I]⁻ [NMe₄]⁺ (**12**[NMe₄]⁺) gave the hexyl phenol **9**[NMe₄]⁺ [1].

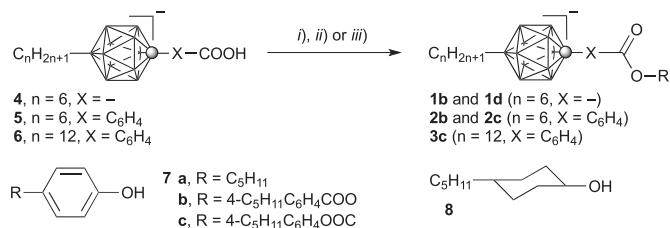
Preparation of iodo acid **11**[NMe₄]⁺ and iodo phenol **12**[NMe₄]⁺ is described elsewhere [1] and involves arylation of [closo-1-CB₁₁H₁₁-12-I]⁻ [NMe₄]⁺ (**13**[NMe₄]⁺) with substituted iodobenzene through a carbonylcopper reagent, followed by deprotection of acid or phenol functionality (Scheme 3).

Phenol **7c** (Scheme 1) was obtained according to a literature procedure [17], while synthesis of **7b** was reported before [18].

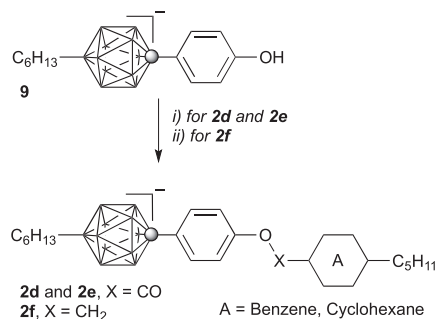
2.2. Liquid crystalline properties

Transition temperatures for compounds **1**[Pyr] and **2**[Pyr] are shown in Table 1. Phase structures were assigned by comparison of POM results with published textures for reference compounds [19].

Compounds in series **2**[Pyr] and **3c**[Pyr] exhibit a SmA phase identified by the characteristic textures observed in polarized light (Fig. 2a). In ester **2e**[Pyr] and ether **2f**[Pyr] the smectic phase is enantiotropic with a tendency for supercooling (Fig. 3a), while in the remaining esters the SmA phase is monotropic appearing as much as 26 K below melting for ester **2d**[Pyr] (Table 1). Compounds in series **1**[Pyr], including the newly synthesized phenyl benzoates **1b**[Pyr] and **1d**[Pyr], exhibit similar phase behavior. Surprisingly, ester **1b**[Pyr] also displays a nematic phase above presumably a SmA phase. The former phase was observed in a supercooled



Scheme 1. Reagents and conditions: i) (COCl)₂, cat. DMF, CH₂Cl₂; ii) ROH **7**, Pyr, CH₂Cl₂, rt; iii) ROH **8**, Pyr, 90 °C, 2 d.



Scheme 2. Reagents and conditions: i) C₅H₁₁-A-COCl, Pyr, CH₂Cl₂; ii) C₅H₁₁-Chx-CH₂OTs (**10**), K₂CO₃, DMF.

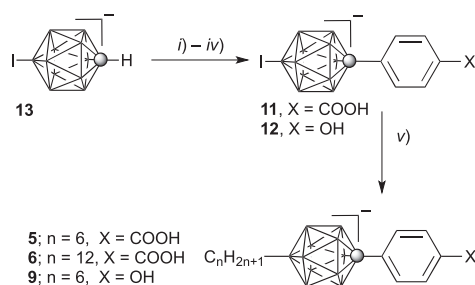
microdroplet (Fig. 2b), while the second phase was detected in some DSC scans (Fig. 3b). Nematic phase is rarely observed in ILC and ion pair **1b**[Pyr] represent the second example of a nematic ILC found among boron cluster derivatives [11].

Analysis of data in Table 1 demonstrates that moving the carboxylic group from the {closo-CB₁₁} cluster in **1a**[Pyr] to the benzene ring lowers the melting point by 70 K in **2c**[Pyr]. Inversion of the direction of the carboxyl group in **2c**[Pyr] significantly increases stability of the SmA by 47 K in **2e**[Pyr]. In contrast, the same change of the COO group orientation in the benzene analogues **2b**[Pyr] and **2d**[Pyr] and also in **1b**[Pyr] and **1d**[Pyr] results in a much smaller increase of mesophase stability by 8 K and 22 K, respectively.

Replacement of the COO group in **2e**[Pyr] with the CH₂O group in **2f**[Pyr] has little effect on the phase stability but significantly lowers the melting point by 31 K.

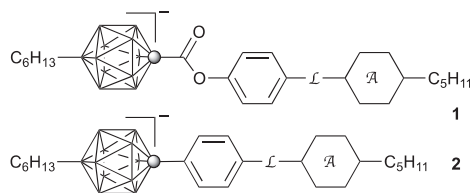
Compounds with the cyclohexyl ring appear to exhibit more stable SmA phase than their benzene analogues. Thus, replacement of the benzene ring with the cyclohexyl ring moderately increases the SmA-I transition in the pair **2b**[Pyr] and **2c**[Pyr], while the same replacement in pairs **1d**[Pyr] and **1e**[Pyr], and **2d**[Pyr] and **2e**[Pyr] stabilizes the SmA phase by 46 K and 57 K, respectively.

A comparison of the clearing temperatures *T*_c in series **1**[Pyr] and **2**[Pyr] shows that insertion of a COO group between the {closo-1-CB₁₁} and Ph groups increases stability of the mesophase by an



Scheme 3. Reagents and conditions: i) BuLi, THF; ii) Cul; iii) I-C₆H₄-X', Pd(OAc)₂, (o-MeOC₆H₄)₃P; iv) deprotection X' → X; v) C_nH_{2n+1}ZnCl, Pd₂(dba)₃, [HPCy₃]⁺[BF₄]⁻, THF.

Table 1
Transition temperatures (°C) and enthalpies (kJ/mol, in parentheses) for **1[Pyrr]** and **2[Pyrr]**.^a



L	A	1[Pyrr]	2[Pyrr]
–	a	Chx Cr ₁ 162 Cr ₂ 178 I ^b (9.8) (24.3)	NA
–COO–	b	Ben Cr 104 (SmX 87 N 93) ^{c,d} I (64.4) (0.7) (1.7)	Cr 92 (SmA 75) ^c I (59.6) (1.0)
	c	Chx NA	Cr 108 (SmA 92) ^e I ^e (45.4) (3.9)
–OOC–	d	Ben Cr 125 (SmA 115) ^{c,f} I (44.7)	Cr 109 (SmA 83) ^f I (72.7) (3.6)
	e	Chx Cr ₁ 109 Cr ₂ 119 SmA 161 I ^b (7.7) (14.9) (6.2)	Cr 136 SmA 139 I (56.9) ^g
–OCH ₂ –	f	Chx NA	Cr 105 SmA 141 I ^e (40.9) (7.7)

^a Transition temperatures obtained on heating.

^b Ref. [11].

^c Monotropic transition.

^d Obtained on cooling.

^e Ref. [1].

^f Optical determination.

^g Combined enthalpy.

average of 22 K with the smallest effect for the **1b[Pyrr]/2b[Pyrr]** pair ($\Delta T_C = 18$ K) and the largest for the **1d[Pyrr]/2d[Pyrr]** pair ($\Delta T_C = 32$ K).

Increasing the chain length has a desired effect on thermal properties of the ILC: it lowers the melting point by 37 K and increases stability of the SmA phase by 45 K leading to a broad range enantiotropic mesophase (Fig. 4). This change is presumably due to better matching of the length of substituents at the B(12) and C(1) positions of the {*closo*-CB₁₁} cluster and consequently better filling space in head-to-tail molecular arrangement in the SmA phase in **3c** than in **2c**.

Structure–property relationships found in series **1[Pyrr]** and **2[Pyrr]** are consistent with trends observed for the N–I transition in non-ionic structurally related calamitic mesogens of the general structure **14** (Fig. 5) [20]. Thus, statistical analysis of the difference in T_{NI} for 16 pairs of isostructural mesogenic esters **14a** and **14b**, and four pairs of ethers **14c** shows that replacement of the benzene ring with cyclohexane increases the nematic phase stability by 18 ± 8 K, 20 ± 7 K and 46 ± 2 K, respectively. On the other hand, changing orientation of the ester group from ester of phenol to ester of

cyclohexanol or replacement of the ArOCH₂ group with a ArOOC group in cyclohexane derivatives **14d** and **14e**, significantly increases the N phase stability by about 40 K. Similarly, in isostructural analogues of *p*-carborane **15**, that are closely related to **2d** and **2e**, the cyclohexyl derivative **15a** exhibits higher stability of the nematic phase by 16 K than its benzene analogue **15b** (Fig. 6) [21]. Finally, inserting a COO group between 4-pentylbicyclo[2.2.2]octane group and benzene ring in **14f** increases the mesophase stability by 21 ± 8 K, which is nearly identical to that observed for three pairs **1[Pyrr]/2[Pyrr]**.

3. Summary and conclusions

We have demonstrated that [*closo*-1-CB₁₁H₁₁-1-Ph][–] group is a viable structural element of ionic liquid crystals. The removal of the esters linking group between the cluster and the benzene ring in series **1[Pyrr]** destabilizes the mesophase by about 20 K, but leads to more chemically stable derivatives, such as **2f[Pyrr]** that are resistant to hydrolytic conditions. Increasing the length of the chain has a favorable effect on phase stability and range, which is important for further optimization of properties.

Structure–property relationships observed in series **1[Pyrr]** and **2[Pyrr]** follow those established for non-ionic liquid crystals, which provides good design tool for new mesogens with desired properties.

4. Experimental section

4.1. General procedures

NMR spectra were obtained at 400 MHz (¹H) and 128 MHz (¹³B) in CD₃CN. Chemical shifts were referenced to the solvent (δ ¹H, 1.93 ppm) or to an external sample of B(OH)₃ in MeOH (δ ¹³B, 18.1 ppm). Mass spectrometry was acquired in the ESI mode. Optical microscopy and phase identification was performed using a PZO “Biolar” polarized microscope equipped with a HCS250 Instec hot stage. Thermal analysis was obtained using a TA Instruments 2920 DSC. Transition temperatures (onset) and enthalpies were obtained using small samples (0.3–1 mg) and a heating rate of 5 K min^{–1} under a flow of nitrogen gas. For DSC and combustion analyses, each compound was additionally purified by filtering solutions in CH₂Cl₂ to remove particles, followed by recrystallization from appropriate solvent until constant transition temperatures. The resulting crystals were dried in vacuum at ambient temperature.

4.2. Synthesis of esters **1[NEt₄]**–**3c[NEt₄]**. General procedure

4.2.1. Method A

[*closo*-1-CB₁₁H₁₀-1-COOH-12-C₆H₁₃][–][NEt₄]⁺ (**4[NEt₄]**) [11].
[*closo*-1-CB₁₁H₁₀-1-C₆H₄COOH-12-C₆H₁₃][–][NEt₄]⁺ (**5[NEt₄]**) [1] or

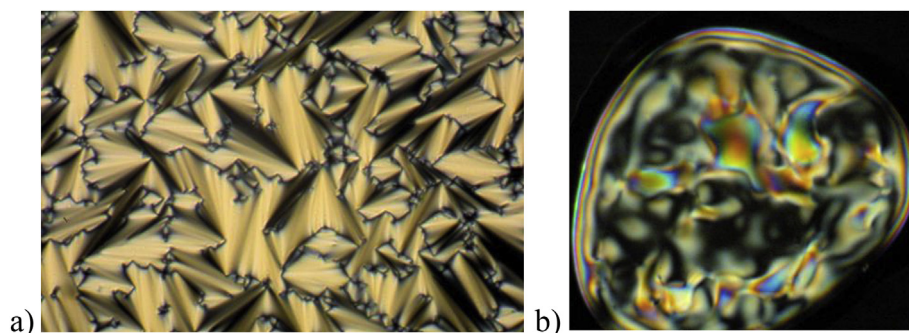


Fig. 2. Optical textures of a SmA phase for **2f[Pyrr]** (a) and a nematic phase for **1b[Pyrr]** in a supercooled microdroplet (b). Magnification $\times 50$.

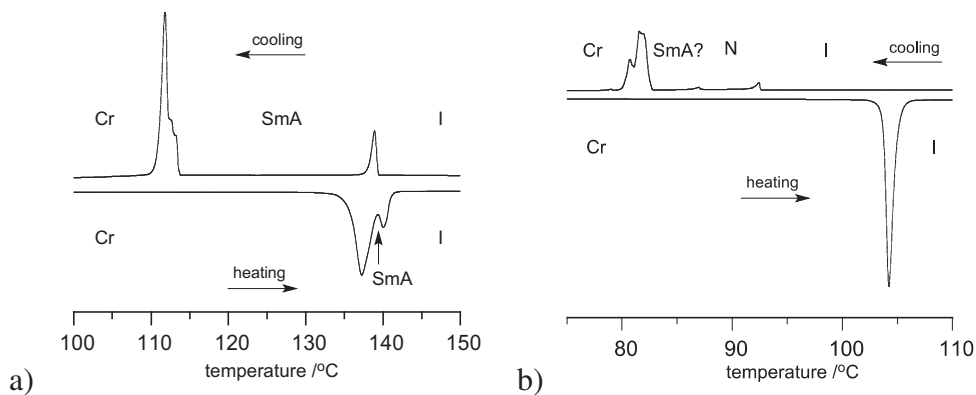


Fig. 3. DSC trace of ester a) **2e[Pyr]** and b) **1b[Pyr]**; heating rate 5 K min⁻¹.

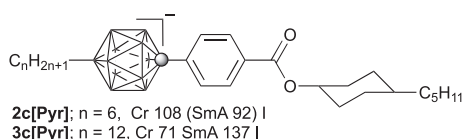


Fig. 4. A comparison of the transition temperatures for two homologues.

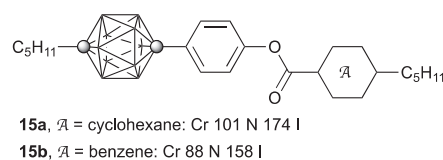
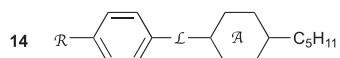


Fig. 6. A comparison of the transition temperatures for two isostructural analogues.

[*closo*-1-CB₁₁H₁₀-1-C₆H₄COOH-12-C₁₂H₂₅]⁻ [NMe₄]⁺ (**6[NET₄]**) (0.12 mmol) was dissolved in CH₂Cl₂ (2 mL), oxalyl chloride (COCl)₂ (226 mg, 1.78 mmol) and catalytic amounts of DMF were added. The reaction mixture was stirred for 30 min and volatiles were removed *in vacuo*. For the preparation of phenol esters **1b[NET₄]**, **1d[NET₄]**, **2b[NET₄]**, crude acid chloride was dissolved in CH₂Cl₂ (1 mL), pyridine (24 mg, 0.3 mmol) was added followed by phenol **7** (0.12 mmol) and stirred at ambient temperature overnight. For the preparation of esters **2c[NET₄]** and **3c[NET₄]**, the acid chloride was dissolved in pyridine (48 mg, 0.6 mmol), *trans*-pencylcyclohexanol [**12**] (102 mg, 0.6 mmol) was added and the reaction mixture was stirred at 90 °C for 2 days followed by removal of volatiles *in vacuo*. The resulting reaction mixture was diluted with CH₂Cl₂ and washed twice with 10% HCl. The organic layer was separated, and the aqueous layer was extracted (CH₂Cl₂). Combined CH₂Cl₂ layers were dried (Na₂SO₄) and solvent evaporated giving a white crystalline solid of esters as the [NET₄]⁺ salt. The crude ion pair was passed through a silica gel plug (CH₂Cl₂/MeCN, 5:1) and used for the subsequent cation exchange.

4.2.2. Method B

4-Pentylbenzoic acid or *trans*-4-pencylcyclohexanecarboxylic acid (0.15 mmol) was dissolved in excess SOCl₂ (1 mL), stirred at 75 °C for 2 h and evaporated to dryness *in vacuo*. The resulting crude acid chloride was dissolved in anhydrous CH₂Cl₂ (2 mL), pyridine (24 mg, 0.30 mmol) and [*closo*-1-CB₁₁H₁₀-1-C₆H₄OH-12-



- 14** R—C₆H₄—L—A—C₅H₁₁
- a, L = OOC, A Chx vs Ben: ΔT_{NI} = 18±8 K, n = 16
 b, L = COO, A Chx vs Ben: ΔT_{NI} = 20±7 K, n = 16
 c, L = OCH₂, A Chx vs Ben: ΔT_{NI} = 46±2 K, n = 4
 d, A = Chx, L COO vs OOC: ΔT_{NI} = 38±5 K, n = 6
 e, A = Chx, L OOC vs OCH₂: ΔT_{NI} = 41±7 K, n = 12
 f, A = BCO, L OOC vs —: ΔT_{NI} = 21±8 K, n = 8

Fig. 5. Statistical analysis of difference in T_{NI} for series of *n* isostructural pairs of mesogens. Chx stands for the cyclohexane ring, Ben for benzene and BCO for bicyclo [2.2.2]octane.

C₆H₁₃]⁻ [NMe₄]⁺ (**9[NME₄]**, 50 mg, 0.13 mmol) were added. After stirring overnight, the reaction was worked up and pure esters were isolated as described in Method A.

4.3. Preparation of 1[Pyr]–3[Pyr]. General procedure

The ion pair **1[NET₄]**, **2[NET₄]** or **3[NET₄]** was dissolved in CH₂Cl₂ and *N*-butyl-4-heptyloxypyridinium bromide [**9**] (2.0 equiv) was added resulting in formation of a precipitate. Water was added and the biphasic system was stirred vigorously until all the precipitate had dissolved. The CH₂Cl₂ layer was separated, and the aqueous layer was extracted with additional CH₂Cl₂. The CH₂Cl₂ layers were combined, dried (Na₂SO₄), evaporated and the resulting product was passed through a short silica gel plug (CH₂Cl₂) giving a white crystalline solid product. Further purification was achieved by repeating recrystallization from EtOH/H₂O mixtures (3–5×), and AcOEt/*n*-hexane mixtures (2×) providing pure product as white crystalline material.

4.3.1. Ester 1b[Pyr]

Obtained in 55% overall yield according to Method A: ¹H NMR (400 MHz, CD₃CN) δ 0.40–2.50 (m, 10H, B–H), 0.47–0.58 (m, 2H, B–CH₂), 0.88 (t, *J* = 6.7 Hz, 3H, CH₃), 0.91 (t, *J* = 6.8 Hz, 6H, CH₃), 0.96 (t, *J* = 7.4 Hz, 3H, CH₃), 1.13–1.41 (m, 20H, CH₂), 1.42–1.50 (m, 2H, CH₂), 1.60–1.68 (m, 2H, CH₂), 1.77–1.92 (m, 4H, CH₂), 2.64 (t, *J* = 7.8 Hz, 2H, Benz–CH₂), 4.29 (t, *J* = 6.7 Hz, 2H, O–CH₂), 4.31 (t, *J* = 8.1 Hz, 2H, N–CH₂), 7.13 (d, *J* = 8.5 Hz, 2H, Benz–H), 7.19 (d, *J* = 8.7 Hz, 2H, Benz–H), 7.28 (d, *J* = 8.5 Hz, 2H, Benz–H), 7.34 (d, *J* = 7.4 Hz, 2H, Pyr–H), 8.17 (d, *J* = 8.7 Hz, 2H, Benz–H), 8.39 (d, *J* = 7.3 Hz, 2H, Pyr–H); ¹³C {¹H} NMR (100 MHz, CD₃CN) δ 13.8, 14.4, 14.5, 14.6, 20.0, 21.2 (br), 23.2, 23.3, 23.6, 26.3, 29.2, 29.6, 31.2, 31.3, 31.7, 32.2, 32.5, 32.9, 33.6, 33.8, 36.6, 60.6, 72.4, 114.8, 123.3, 123.9, 127.7, 129.8, 131.0, 146.4, 149.6, 149.7, 150.8, 163.8, 166.1, 167.6, 171.7. Anal. Calcd for C₄₂H₇₀B₁₁NO₅: C, 64.02; H, 8.95; N, 1.78. Found: C, 64.32; H, 8.95; N, 1.82.

4.3.2. Ester 1d[Pyr]

Obtained in 56% overall yield according to Method A: ¹H NMR (400 MHz, CD₃CN) δ 0.40–2.50 (m, 10H, B–H), 0.47–0.58 (m, 2H, B–

CH₂), 0.88 (t, *J* = 6.3 Hz, 3H, CH₃), 0.907 (t, *J* = 6.1 Hz, 3H, CH₃), 0.909 (t, *J* = 6.0 Hz, 3H, CH₃), 0.96 (t, *J* = 7.4 Hz, 3H, CH₃), 1.13–1.41 (m, 20H, CH₂), 1.42–1.50 (m, 2H, CH₂), 1.67 (quint, *J* = 7.4 Hz, 2H, CH₂), 1.75–1.92 (m, 4H, CH₂), 2.72 (t, *J* = 7.7 Hz, 2H, Benz-CH₂), 4.29 (t, *J* = 6.6 Hz, 2H, O-CH₂), 4.31 (t, *J* = 7.4 Hz, 2H, N-CH₂), 7.06 (d, *J* = 8.9 Hz, 2H, Benz-H), 7.24 (d, *J* = 8.9 Hz, 2H, Benz-H), 7.34 (d, *J* = 7.5 Hz, 2H, Pyr-H), 7.40 (d, *J* = 8.3 Hz, 2H, Benz-H), 8.08 (d, *J* = 8.2 Hz, 2H, Benz-H), 8.39 (d, *J* = 7.5 Hz, 2H, Pyr-H). Anal. Calcd for C₄₂H₇₀B₁₁NO₅: C, 64.02; H, 8.95; N, 1.78. Found: C, 64.20; H, 8.91; N, 1.87.

4.3.3. Ester **2b**[Pyr]

Obtained in 47% overall yield according to Method A: ¹H NMR (400 MHz, CD₃CN) δ 0.40–2.50 (m, 10H, B-H), 0.50–0.55 (m, 2H, B-CH₂), 0.88 (t, *J* = 6.9 Hz, 3H, CH₃), 0.91 (t, *J* = 6.8 Hz, 6H, CH₃), 0.96 (t, *J* = 7.4 Hz, 3H, CH₃), 1.15–1.53 (m, 22H, CH₂), 1.64 (quint, *J* = 7.5 Hz, 2H, CH₂), 1.80–1.92 (m, 4H, CH₂), 2.64 (t, *J* = 6.6 Hz, 2H, Benz-CH₂), 4.29 (t, *J* = 6.6 Hz, 2H, O-CH₂), 4.31 (t, *J* = 7.5 Hz, 2H, N-CH₂), 7.11 (d, *J* = 8.5 Hz, 2H, Benz-H), 7.27 (d, *J* = 8.4 Hz, 2H, Benz-H), 7.34 (d, *J* = 7.5 Hz, 2H, Pyr-H), 7.69 (d, *J* = 8.6 Hz, 2H, Benz-H), 7.92 (d, *J* = 8.6 Hz, 2H, Benz-H), 8.39 (d, *J* = 7.5 Hz, 2H, Pyr-H); ¹³C{¹H} NMR (100 MHz, CD₃CN) δ 13.7, 14.3, 14.4, 14.5, 19.9, 21.0 (br), 23.2, 23.3, 23.5, 26.2, 29.1, 29.5, 31.2, 32.0, 32.2, 32.4, 32.8, 33.5, 33.7, 35.8, 60.5, 72.3, 114.8, 122.5, 122.8, 128.3, 130.3, 132.5, 141.8, 146.4, 149.9, 156.2, 165.4, 167.0, 171.6; ¹¹B{¹H} NMR (128 MHz, CD₃CN) δ –13.4 (5B), –11.6 (2B), 3.9 (br, 1B). Anal. Calcd for C₄₁H₇₀B₁₁NO₃: C, 66.20; H, 9.48; N, 1.88. Found: C, 66.52; H, 9.42; N, 1.91.

4.3.4. Ester **2d**[Pyr]

Obtained in 62% overall yield according to Method B: ¹H NMR (400 MHz, CD₃CN) δ 0.4–2.5 (m, 10H, B-H), 0.45–0.55 (m, 2H, B-CH₂), 0.88 (t, *J* = 7.1 Hz, 3H, CH₃), 0.91 (t, *J* = 6.7 Hz, 3H, CH₃), 0.91 (t, *J* = 6.7 Hz, 3H, CH₃), 0.96 (t, *J* = 7.3 Hz, 3H, CH₃), 1.13–1.53 (m, 22H, CH₂), 1.59–1.68 (m, 2H, CH₂), 1.64 (quint, *J* = 7.5 Hz, 2H, CH₂), 1.86–1.92 (m, 4H, CH₂), 2.64 (t, *J* = 7.6 Hz, 2H, Benz-CH₂), 4.29 (t, *J* = 6.6 Hz, 2H, O-CH₂), 4.31 (t, *J* = 7.5 Hz, 2H, N-CH₂), 7.11 (d, *J* = 8.5 Hz, 2H, Benz-H), 7.27 (d, *J* = 8.4 Hz, 2H, Benz-H), 7.34 (d, *J* = 7.5 Hz, 2H, Pyr-H), 7.69 (d, *J* = 8.6 Hz, 2H, Benz-H), 7.92 (d, *J* = 8.6 Hz, 2H, Benz-H), 8.39 (d, *J* = 7.5 Hz, 2H, Pyr-H); ¹¹B{¹H} NMR (128 MHz, CD₃CN) δ –13.4 (5B), –11.6 (5B), 3.9 (br, 1B). Anal. Calcd for C₄₁H₇₀B₁₁NO₃: C, 66.20; H, 9.48; N, 1.88. Found: C, 66.42; H, 9.46; N, 1.85.

4.3.5. Ester **2e**[Pyr]

Obtained in 87% overall yield according to Method B: ¹H NMR (400 MHz, CD₃CN) δ 0.4–2.5 (m, 10H, B-H), 0.45–0.55 (m, 2H, B-CH₂), 0.87–0.93 (m, 6H, CH₃), 0.88 (t, *J* = 6.9 Hz, 3H, CH₃), 0.96 (t, *J* = 7.4 Hz, 3H, CH₃), 0.98–1.06 (m, 2H, CH₂), 1.12–1.59 (m, 29H, CH and CH₂), 1.80–1.91 (m, 6H, CH₂), 2.09–2.12 (m, 2H, CH₂), 2.46 (tt, *J*₁ = 12.2 Hz, *J*₂ = 3.6 Hz, 1H, CH-COO), 4.29 (t, *J* = 6.9 Hz, 2H, O-CH₂), 4.31 (t, *J* = 7.5 Hz, 2H, N-CH₂), 6.81 (d, *J* = 8.8 Hz, 2H, Benz-H), 7.33 (d, *J* = 7.5 Hz, 2H, Pyr-H), 7.50 (d, *J* = 8.8 Hz, 2H, Benz-H), 8.39 (d, *J* = 7.5 Hz, 2H, Pyr-H); ¹¹B{¹H} NMR (128 MHz, CD₃CN) δ –13.3 (5B), –11.7 (5B), 3.4 (1B). Anal. Calcd for C₄₁H₇₆B₁₁NO₃: C, 65.66; H, 10.21; N, 1.87. Found: C, 65.77; H, 10.20; N, 1.94.

4.3.6. Ester **3c**[Pyr]

Obtained in 28% overall yield according to Method A: ¹H NMR (400 MHz, CD₃CN) δ 0.40–2.50 (m, 10H, B-H), 0.50–0.63 (m, 2H, B-CH₂), 0.86–0.92 (m, 9H, CH₃), 0.96 (t, *J* = 7.4 Hz, 3H, CH₃), 1.00–1.11 (m, 2H, CH₂), 1.13–1.41 (m, 37H, CH and CH₂), 1.42–1.52 (m, 4H, CH₂), 1.78–1.92 (m, 6H, CH₂), 2.00–2.08 (m, 2H, CH₂), 4.29 (t, *J* = 6.6 Hz, 2H, O-CH₂), 4.31 (t, *J* = 7.5 Hz, 2H, N-CH₂), 4.81 (tt, *J*₁ = 11.1 Hz, *J*₂ = 4.4 Hz, 1H, CH-OOC), 7.34 (d, *J* = 7.5 Hz, 2H, Pyr-H), 7.59 (d, *J* = 8.6 Hz, 2H, Benz-H), 7.74 (d, *J* = 8.5 Hz, 2H, Benz-H), 8.39

(d, *J* = 7.4 Hz, 2H, Pyr-H); ¹³C{¹H} NMR (100 MHz, CD₃CN) δ 13.7, 14.36, 14.39, 14.41, 19.9, 23.3, 23.38, 23.40, 26.2, 27.6, 29.1, 29.5, 30.1, 30.39, 30.44, 30.50, 30.56, 31.5, 31.7, 32.39, 32.42, 32.7, 32.9, 33.52, 34.1, 37.3, 37.4, 60.6, 72.3, 74.9, 114.8, 129.2, 129.9, 146.4, 147.7, 166.4, 171.7. Anal. Calcd for C₄₇H₈₈B₁₁NO₃: C, 67.68; H, 10.63; N, 1.68. Found: C, 67.96; H, 10.52; N, 1.76.

4.4. [closo-1-CB₁₁H₁₀-1-C₆H₄COOH-12-C₁₂H₂₅][−] [NEt₄]⁺ (**6**[NEt₄])

To a solution of anhydrous ZnCl₂ (2.10 g, 15.4 mmol) in anhydrous THF (6 mL) under Ar was added C₁₂H₂₅MgBr (14.3 mL, 14.3 mmol, 1.0 M in Et₂O) at 0 °C forming a white, thick slurry, which was stirred for 15 min. Anhydrous NMP (6 mL), Pd₂(dba)₃·CHCl₃ (24.6 mg, 2 mol %), and, [HPCy₃](BF₄) (35.1 mg, 8 mol %) were then added and the reaction mixture turned dark green but slowly faded to red/orange. After 5 min, [closo-1-CB₁₁H₁₀-1-[4-C₆H₄COOH]-12-I][−] [NMe₄]⁺ [**1**] (**11**[NMe₄], 583 mg, 1.18 mmol) was added, and the reaction mixture was stirred at 90 °C until ESI-MS spectrum of a small aliquot (quenched in sat. NH₄Cl and extracted into AcOEt) showed complete conversion to product (about 24 h; if not completed, the palladium source and ligand were further added.). Sat. NH₄Cl (50 mL) was added and the remaining aqueous layer was extracted with Et₂O twice. The organic layers were combined, dried over Na₂SO₄, and solvent was removed giving a black sludge. This material was purified by column chromatography (SiO₂, CH₂Cl₂/CH₃CN 9:1 then CH₂Cl₂/CH₃CN/MeOH 9:3:1). The purity of fractions was confirmed by TLC and ESI-MS analyses. The resulting product was dissolved in AcOEt the solution was washed with 1 N HCl (×2), then with aq. Et₄NBr twice, and dried (Na₂SO₄). The solvent was removed, and the resulting material was dried *in vacuo* giving 426 mg (64% yield) of the 12-dodecyl acid **6**[NEt₄] as a pale solid material: ¹H NMR (400 MHz, CD₃CN) δ 0.40–2.50 (m, 10H, B-H), 0.48–0.57 (m, 2H, B-CH₂), 0.89 (t, *J* = 6.8 Hz, 3H, CH₃), 1.15–1.35 (m, 32H, CH₂), 3.17 (q, *J* = 7.3 Hz, 8H, CH₂), 7.60 (d, *J* = 8.6 Hz, 2H, Benz-H), 7.76 (d, *J* = 8.6 Hz, 2H, Benz-H); ¹³C{¹H} NMR (124.5 MHz, acetone-*d*₆) δ 7.7, 14.4, 21.2 (br), 23.3, 29.4, 30.09, 30.16, 30.31, 30.39, 30.46, 30.54, 30.63, 30.68, 32.6, 53.0 (t, *J*_{CN} = 3.0 Hz), 129.2, 129.3, 129.5, 148.3, 167.5; ¹¹B{¹H} NMR (128 MHz, CD₃CN) δ –13.3 (5B), –11.6 (5B), 3.4 (br, 1B); ¹¹B{¹H} NMR (159 MHz, acetone-*d*₆) δ –12.9 (5B), –11.1 (5B), 4.0 (1B); ESI-MS, *m/z* 431 (M, 100%). Anal. Calcd for C₂₈H₆₀B₁₁NO₂: C, 59.87; H, 10.77; N, 2.49. Found: C, 60.26; H, 10.53; N, 2.39.

Acknowledgments

This project was supported by the NSF grant (DMR-1207585) and JSPS KAKENHI (S) (No. 24229001) (to M.U.), Grant-in-Aid for Young Scientists (A) (No. 25713001) and Astellas Foundation for Research on Metabolic Disorders (to R.T.).

References

- [1] J. Kanazawa, R. Takita, A. Jankowiak, S. Fujii, H. Kagechika, D. Hashizume, K. Shudo, P. Kaszyński, M. Uchiyama, Angew. Chem. Int. Ed. 51 (2013) 000.
- [2] M. Yoshio, T. Mukai, K. Kanie, M. Yoshizawa, H. Ohno, T. Kato, Adv. Mater. 14 (2002) 351–354; M. Yoshio, T. Kagata, K. Hoshino, T. Mukai, H. Ohno, T. Kato, J. Am. Chem. Soc. 128 (2006) 5570–5577; M. Yoshio, T. Mukai, H. Ohno, T. Kato, J. Am. Chem. Soc. 126 (2004) 994–995.
- [3] T. Ichikawa, M. Yoshio, A. Hamasaki, T. Mukai, H. Ohno, T. Kato, J. Am. Chem. Soc. 129 (2007) 10662–10663.
- [4] S. Yazaki, Y. Kamikawa, M. Yoshio, A. Hamasaki, T. Mukai, H. Ohno, T. Kato, Chem. Lett. 37 (2008) 538–539.
- [5] Y. Grabovskiy, A. Kovalchuk, A. Grydyakina, S. Bugaychuk, T. Mirnaya, G. Klimusheva, Liq. Cryst. 34 (2007) 599–603.
- [6] H. Shimura, M. Yoshio, K. Hoshino, T. Mukai, H. Ohno, T. Kato, J. Am. Chem. Soc. 130 (2008) 1759–1765.

- [7] Y. Abu-Lebdeh, A. Abouimrane, P.-J. Alarco, M. Armand, J. Power Sources 154 (2006) 255–261.
- [8] N. Yamanaka, R. Kawano, W. Kubo, T. Kitamura, Y. Wada, M. Watanabe, S. Yanagida, Chem. Commun. (2005) 740–742.
- [9] B. Ringstrand, H. Monobe, P. Kaszynski, J. Mater. Chem. 19 (2009) 4805–4812.
- [10] J. Pecyna, A. Sivaramamoorthy, A. Jankowiak, P. Kaszyński, Liq. Cryst. 39 (2012) 965–971.
- [11] B. Ringstrand, A. Jankowiak, L.E. Johnson, D. Pocięcha, P. Kaszyński, E. Górecka, J. Mater. Chem. 22 (2012) 4874–4880.
- [12] J. Pecyna; B. Ringstrand; M. Bremer; P. Kaszyński submitted for publication.
- [13] A. Jankowiak, A. Januszko, B. Ringstrand, P. Kaszyński, Liq. Cryst. 35 (2008) 65–77.
- [14] ^{13}C NMR (100 MHz, CD_3CN) δ 13.7, 14.3, 19.8, 23.2, 26.2, 29.0, 29.5, 32.3, 33.6, 60.1, 72.3, 114.7, 146.8, 171.5
- [15] E. Erdik, Tetrahedron 48 (1992) 9577–9648.
- [16] P. Knochel, R.D. Singer, Chem. Rev. 93 (1993) 2117–2188.
- [17] E. Fontes, W.K. Lee, P.A. Heiney, G. Nounesis, C.W. Garland, A. Riera, J.P. McCauley Jr., A.B. Smith III, J. Chem. Phys. 92 (1990) 3917–3929.
- [18] A. Januszko, P. Kaszynski, Liq. Cryst. 35 (2008) 705–710.
- [19] D. Demus, L. Richter, Textures of Liquid Crystals, second ed., VEB, Leipzig, 1980; G.W. Gray, J.W.G. Goodby, Smectic Liquid Crystals-textures and Structures, Leonard Hill, Philadelphia, 1984; I. Dierking, Textures of Liquid Crystals, Wiley-VCH, Weinheim, 2003.
- [20] V. Vill, LiqCryst 5.1 database and references therein.
- [21] K. Ohta, A. Januszko, P. Kaszynski, T. Nagamine, G. Sasnouski, Y. Endo, Liq. Cryst. 31 (2004) 671–682.